Physics in Collision - Stanford, California, June 20-22, 2002

TOP AND HIGGS PHYSICS AT THE TEVATRON

Pierre Savard
University of Toronto and TRIUMF, Toronto, Canada

ABSTRACT

We present a summary of our experimental understanding of the top quark and discuss the significant improvements expected in Run II at the Fermilab Tevatron Collider. We also discuss prospects for a Higgs boson discovery at the Tevatron.

1 Introduction

One of the great unsolved puzzles in particle physics revolves around the generation of mass: how do particles become massive? this question is answered in the context of the Standard Model by the Higgs mechanism, which is evoked to break electroweak symmetry. It predicts the existence of a neutral scalar particle, the yet unobserved Higgs boson.

In the Standard Model, the coupling strength between a fermion and the Higgs boson, the Yukawa coupling, determines the fermion mass, which is not predicted by the theory. For all fermions, this coupling is small, except for one particle: the top quark. The top quark mass is close to the electroweak breaking scale and its Yukawa coupling is within a few percent of unity. Those intriguing characteristics have lead some to speculate that the top quark itself is involved in electroweak symmetry breaking or that its mass is a fundamental parameter of a more basic, underlying theory.

We currently know experimentally very little about both the Higgs boson and the top quark. However, in the next few years, the CDF and DØ experiments at the Fermilab Tevatron Collider will pursue a program of precision measurements of the top quark and will conduct an intensive search for the Higgs boson.

In these proceedings, I will summarize our current experimental understanding of the top quark and discuss the prospects for precision measurements in the coming years. I will then give an overview of the strategies that will be used to search for the Higgs boson.

2 The Top Quark

The top quark was discovered by the CDF and DØ collaborations in 1995[1]. This discovery was not unexpected since the structure of the SM requires that there be an SU(2) partner to the b quark. What did come as a surprise was the top quark's mass: 175 GeV/c^2, about 35 times more massive than the b quark, the heaviest known fermion at the time. Given its mass, many properties of the top quark can be calculated within the Standard Model and are given in Table 1.

An interesting consequence of the very short lifetime of the top quark is that it decays before it has time to hadronize. There are therefore no top hadrons and the top quark can thus be studied as a "free" quark.

Table 1: Top quark in th SM

	simulation
charge	+2/3e
spin	1/2
width	1.4 GeV/c^2
mass	175 GeV/c^2
$BR(t \to Wb)$	$\sim$ 100%
lifetime	$\sim 5 \times 10^{-25} s$

Table 2: Some Run I Measurements

	simulation
$BR(t \to Zq)$	< .33 at 95% CL (CDF [2])
$BR(t \to \gamma q)$	< .03 at 95% CL (CDF [2])
$BR(t \to Hb)$	< .36 at 95% CL[1] (DØ [3])
$\frac{BR(t \to Wb)}{BR(t \to Wq)}$	> .56 at 95% CL (CDF [4])
$t\bar{t}$ spin correlation	κ > -.25 at 68% CL (DØ [5])

2.1 Run 1 Measurements

After the discovery of the top quark, the CDF and DØ collaborations undertook studies aimed at characterizing its properties. Because of the statistically limited data sample available in Run 1, most measurements had large uncertainties, with the notable exception of the top mass (see Table 2 and Figure 1). Therefore, our current experimental understanding of the top quark is still very limited and leaves room for potential surprises.

2.2 Run II Top Physics Program

With the start of Run II at the Tevatron, the era of precision top physics has begun. During this period that started in 2000 and that should extend until the start of the Large Hadron Collider (LHC) at CERN, we expect to collect a clean data sample of over 1000 events where at least one B hadron is identified. Table 3 lists some measurement goals from the CDF and DØ experiments [6, 7]. In the following, I will focus on two of the most important top physics measurements in Run II.

2.2.1 Single Top Production

The top quark discovery relied on the production of $t\bar{t}$ pairs via the strong interaction. Top quarks can also be produced singly, via the electroweak interaction. At

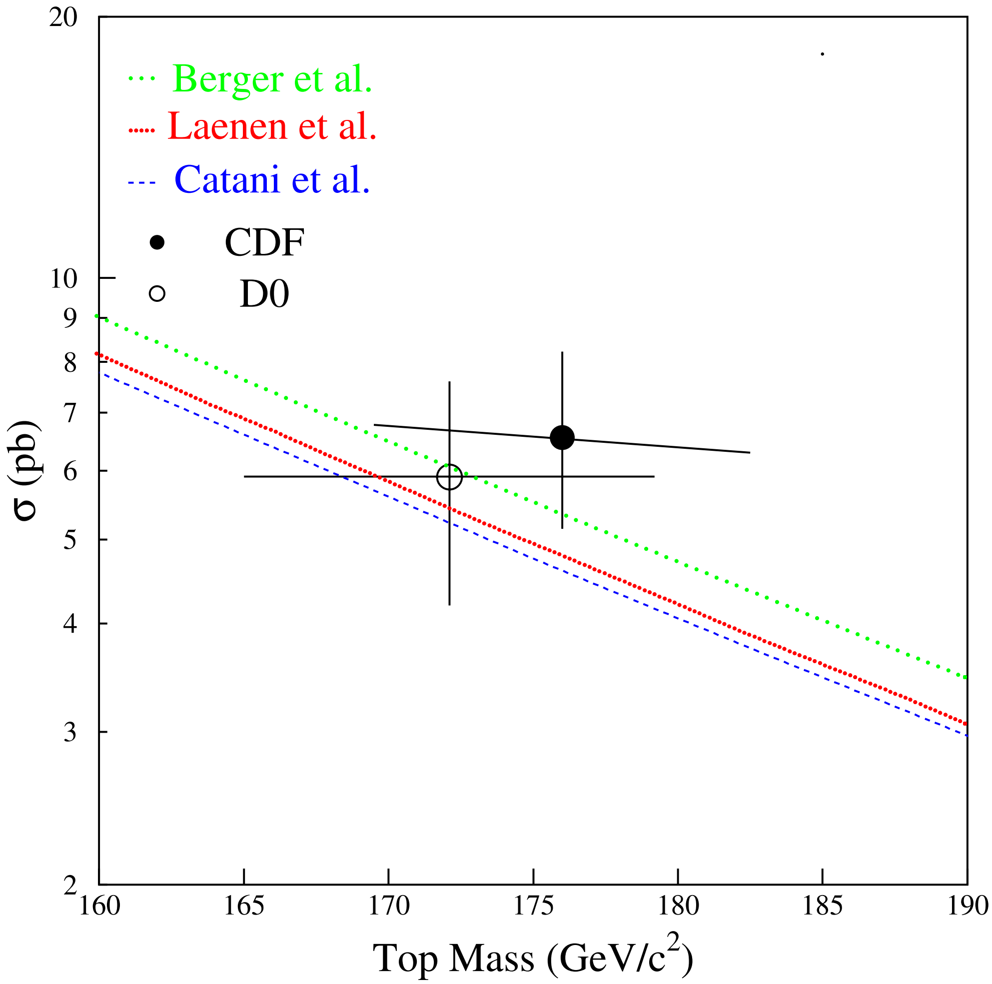

Figure 1: Production cross section and top mass measurements from CDF and D0.

the Tevatron, two production processes dominate: the s-channel W* process, and the t-channel W-gluon fusion process[8]

The single top production cross section is proportional to the CKM matrix element ${V_{tb}}^2$. The measurement of the cross section can thus be interpreted as a measurement of V_{tb}, with fewer assumptions than in branching ratio measurements that can be used to infer V_{tb}[4]. The production cross section can also be sensitive to non-standard couplings of the top quark, making it a very interesting observable to search for new physics[9].

Understanding single top production will also be important for the Tevatron Higgs search since the WH channel, with $H \rightarrow b\bar{b}$, has an identical final state with kinematics very similar to the $W^{\star}$ channel.

Finally, because the single top production proceeds through the V-A inter-

Table 3: Some Top Physics Goals for 2 fb^{-1}

	uncertainty
mass	2-3 GeV/c^2
$t\bar{t}$ cross section	9%
V_{tb}	13%
$BR(t \rightarrow Wb)$	3%
$BR(t \rightarrow Zq)$	$< 1 \times 10^{-2}$
$BR(t \rightarrow \gamma q)$	$< 3 \times 10^{-3}$
BR (W longitudinal)	6%

action, the resulting top quarks are polarized. Since top quarks decay before they hadronize, we should be able to make top quark polarization measurements that have only been made with leptons.

2.2.2 Top Mass Measurement

Precision electroweak measurements have allowed us to probe the effect or radiative corrections on various electroweak observables. Those radiative corrections can exhibit a quadratic dependence on the top quark mass, making this parameter and its experimental error important inputs to global electroweak fits. In fact, our current understanding of the self-consistency of the Standard Model and our knowledge of the Higgs mass are limited by the accuracy to which we currently know the top quark mass[10]. For this reason, reducing the uncertainty on the top quark mass will be one of the top priorities of the Run II physics program.

The goal for the experiments in Run II is to reduce the uncertainty to 2-3 GeV/c^2. Attaining this level of precision will require a large-scale effort to significantly improve our understanding of the jet energy scale and of hard initial and final state QCD radiation. Part of the needed improvements will be made possible with the use of *in situ* calibration samples e.g. the $W \rightarrow jj$ resonance present in $t\bar{t}$ decay or the $Z \rightarrow b\bar{b}$ resonance.

3 Higgs Search at the Tevatron

In the next few years, the Tevatron experiments will have a unique opportunity to find or exclude the SM Higgs boson before the LHC experiments are commissioned.

After a short review of the production and decay properties of the Higgs boson, I will give a summary of the strategies and techniques that will be employed in this ambitious search. A detailed study can be found in the Report of the Tevatron

Higgs Working Group[11].

3.1 Higgs Production and Decay

Figure 2 shows the Higgs production cross section at the Tevatron as a function of the Higgs boson mass. Over the mass range shown, the gluon-gluon fusion process dominates. The cross section for WH and ZH production is lower, but these modes allow for smaller backgrounds and a straightforward trigger signature through the leptonic decay of the weak bosons. The $Ht\bar{t}$ mode has a spectacular decay signature with two W bosons and 4 b quarks but suffers from a very small cross section.

Figure 3 shows the Higgs branching ratio as a function of Higgs mass. Two mass ranges can be identified: the low-mass range where the dominant Higgs decay mode is to a pair of b quarks and the high-mass range where the Higgs decays to a pair of W bosons. Different experimental strategies have been developed to deal with these two mass regimes.

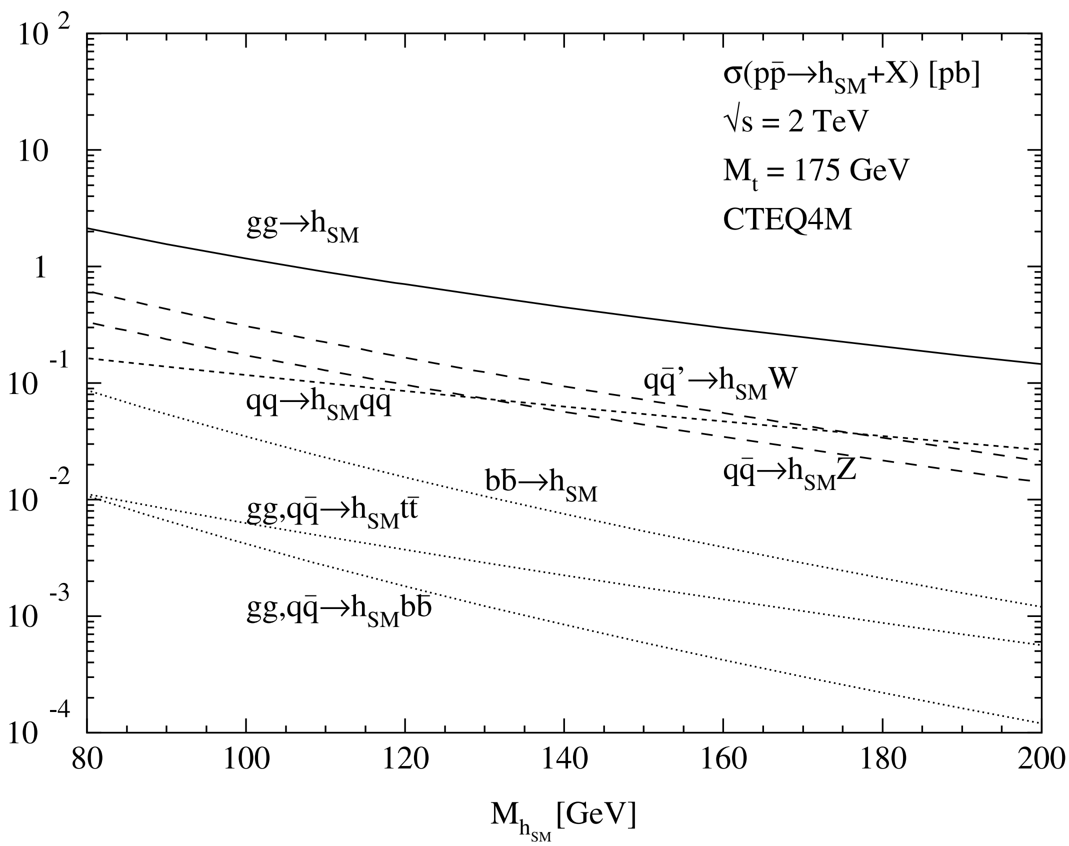

Figure 2: Higgs production cross section versus Higgs mass for various production processes.

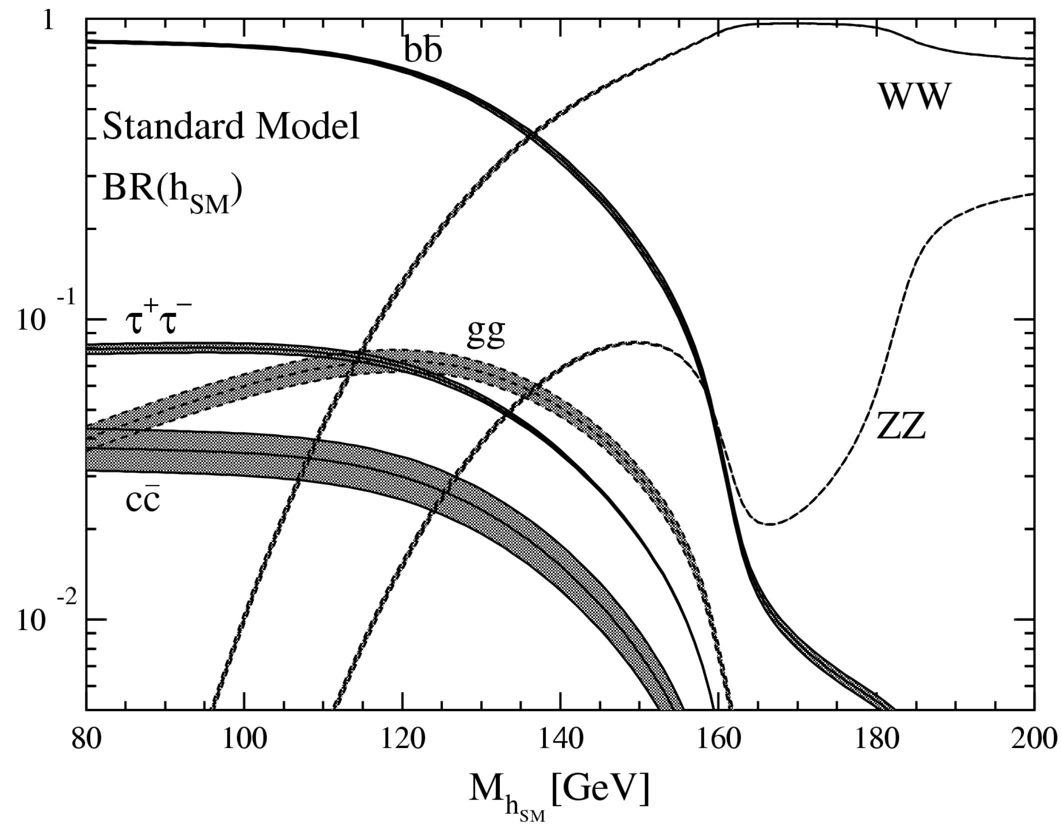

Figure 3: Higgs branching ratios versus Higgs mass.

3.1.1 Experimental Tools

As mentioned above, the low-mass regime is dominated by Higgs decays to $b\bar{b}$. In order to maximize the search sensitivity, we will need to optimize B tagging efficiency and improve dijet mass resolution.

To observe a $H \rightarrow b\bar{b}$ resonance that is as narrow as possible in the background-dominated dijet mass spectrum, we need to make improvements in the jet energy resolution. To this effect, CDF developed in Run I a technique that makes use of tracking, preshower, and shower maximum detectors to improve its energy resolution. It is hoped that both detectors will be able to achieve a $H \rightarrow b\bar{b}$ mass resolution of about 10%.

The two experiments have much improved tracking systems for Run II. The D∅ detector now has a large silicon vertex detector surrounded by a fiber tracker. The two devices are immersed in a 2 Tesla magnetic field. CDF replaced its drift chamber and its silicon vertex detector which now has an acceptance that extends to $|\eta| < 2$. These improvements will translate into significantly higher b-tagging efficiencies relative to what was obtained in Run I. The results that will be presented later assumed a tight b-tag efficiency of 60% and a loose b-tag efficiency of 75%, while keeping the fake rate under 1%.

The Tevatron Higgs Working Group studied potential improvements that could be made by using neural networks, which have been extensively used by the LEP experiments in their Higgs searches. The outcome of the study was very promising and a neural net analysis was used to obtain the results presented in Figure 4.

Before the Higgs search attains the sensitivity required for an observation, we will be searching for two Standard Model signals that have not yet been observed: single top in the $W^\star$ channel and WZ, with $Z \to b\bar{b}$. Both these channels have the same final state with similar kinematics as the WH channel but have significantly higher $\sigma \times BR$. This will provide opportunities to exercise analysis tools and estimate background rejection techniques well before a Higgs signal becomes visible.

3.2 Results from Tevatron Higgs Working Group

3.2.1 Low Mass Range

Results from the WH and ZH channels with $H \to b\bar{b}$ and the leptonic decay of the weak bosons are presented in Table 4. One jet from the Higgs decay is required to be tagged by a "tight" algorithm and the other jet by a "loose" algorithm whose efficiencies were mentioned earlier. The main backgrounds come from $t\bar{t}$, $Wb\bar{b}$, single top, and WZ.

3.2.2 High Mass Range

The high mass region is dominated by the Higgs decay to $WW^\star$ and WW. In this case, one can afford to make use of the gluon fusion production mechanism that has a higher cross section. However, the results below also use the associated Higgs production mechanism since it can provide striking trilepton signatures. The main backgrounds come from WW, WZ, ZZ, and $t\bar{t}$. The results of the study are presented in Table 5.

3.2.3 Combined Results

The integrated luminosity required to observe or exclude a Higgs Boson as a function of Higgs mass is shown in Figure 4. The study finds that a SM Higgs with a mass up to 135 GeV/c^2 can be excluded at 95% CL with 6 fb^{-1} and up to 180 GeV/c^2 with 10 fb^{-1}. With 15 fb^{-1}, one could obtain 3 σ "evidence" up to 135 GeV/c^2.

Table 4: Low-mass Higgs search sensitivities per detector in 1 fb^{-1}

		Higgs Mass (GeV/c^2)				
Channel	Rate	90	100	110	120	130
	S	8.7	9.0	4.8	4.4	3.7
$\ell\nu b\bar{b}$	B	28	39	19	26	46
	$S/\sqrt{B}$	1.6	1.4	1.1	0.9	0.5
	S	12	8	6.3	4.7	3.9
$\nu\nu b\bar{b}$	B	123	70	55	45	47
	$S/\sqrt{B}$	1.1	1.0	0.8	0.7	0.6
	S	1.2	0.9	0.8	0.8	0.6
$\ell\ell b\bar{b}$	B	2.9	1.9	2.3	2.8	1.9
	$S/\sqrt{B}$	0.7	0.7	0.5	0.5	0.4

Table 5: High-mass Higgs search sensitivities per detector in 1 fb^{-1}

		Higgs Mass (GeV/c^2)						
Channel	Rate	120	130	140	150	160	170	180
	S	-	-	2.6	2.8	1.5	1.1	1.0
$\ell\ell\nu\nu$	B	-	-	44	30	4.4	2.4	3.8
	$S/\sqrt{B}$	-	-	0.39	0.51	0.71	0.71	0.51
	S	0.08	0.15	0.29	0.36	0.41	0.38	0.26
$jj\ell\ell$	B	0.58	0.58	0.58	0.58	0.58	0.58	0.58
	$S/\sqrt{B}$	0.11	0.20	0.38	0.47	0.54	0.50	0.34

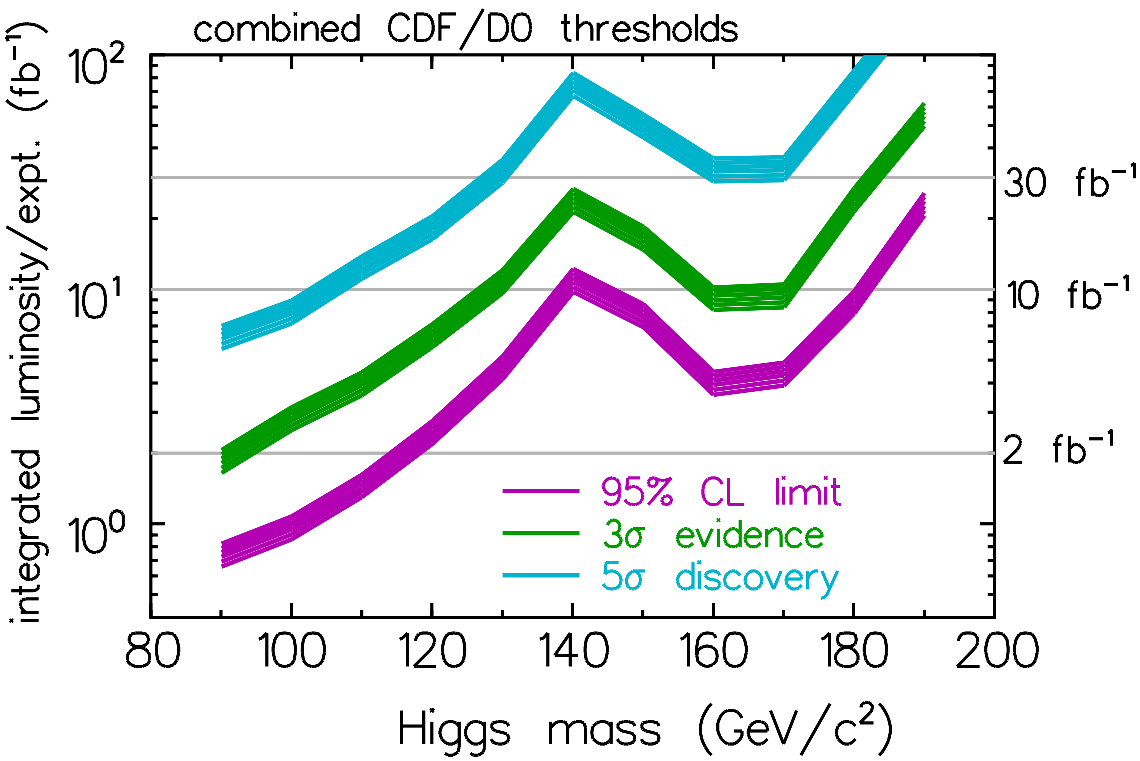

Figure 4: Integrated luminosity required to observe or exclude a Higgs boson versus Higgs mass.

The study assumed a $b\bar{b}$ dijet mass resolution of 10%, b-tagging efficiencies of 75% on one of the B hadrons (tight algorithm), and 60% on the other (loose algorithm). Acceptance and efficiencies for signal and backgrounds were estimated using a Monte Carlo simulation that parameterized the response of a generic Run II detector. The size of the bands on Figure 4 reflect a 30% uncertainty that includes b-tagging, mass resolution, background rate and other effects.

4 Conclusion

With the beginning of Run II at the Tevatron, the era of precision top physics has begun and the hunt for the Higgs boson has resumed. This exciting period will be followed with the commissioning of the LHC, a true "top quark factory". The measurements made in the next decade should allow us to determine whether the generation of mass for elementary particles is indeed described by the Higgs mechanism of the Standard Model and whether the top quark plays a special role in the breaking of electroweak symmetry.

References

1. F. Abe *et al*, Phys. Rev. Lett. **74**, 2626 (1995); B. Abachi *et al*, Phys. Rev. Lett. **74**, 2632 (1995).
2. F. Abe *et al*, Phys. Rev. Lett. **80**, 2525 (1998).
3. B. Abbott *et al*, Phys. Rev. Lett. **88**, 151803 (2002).
4. T. Affolder *et al*, Phys. Rev. Lett. **86**, 3233-3238 (2001).
5. B. Abbott *et al*, Phys. Rev. Lett. **85**, 256-261 (2000).
6. DØ Collaboration, FERMILAB-PUB-00-357-E, October 1996.
7. CDF Collaboration, FERMILAB-PUB-00-390-E, November 1996.
8. B.W. Harris *et al*, FERMILAB-PUB-02-134-T, hep-ph/0207055, July 2002.
9. T. Tait, C.P. Yuan, Phys. Rev. **D63**, 014018 (2001).
10. F. Teubert, these proceedings.
11. M. Carena *et al*, FERMILAB-CONF-00-279-T, October 2000.